catalysts

MDPI

Article

Catalytic Microwave-Assisted Pyrolysis of the Main Residue of the Brewing Industry

Fernanda Pimenta, Elmis Filho, Ângelo Diniz and Marcos A. S. Barrozo *

Chemical Engineering School, Federal University of Uberlândia, Uberlândia 38408-100, Brazil; fernandapimentasssp@hotmail.com (F.P.); elmisfilho@hotmail.com (E.F.); af.diniz@ufu.br (Â.D.)
* Correspondence: masbarrozo@ufu.br; Fax: +55-34-32394188

Abstract: Most agro-industrial wastes are lignocellulosic biomass. Several technologies have been developed to convert these residues to value-added products. Among these processes, pyrolysis refers to the thermal degradation of organic materials. Microwave-assisted pyrolysis (MAP) is more advantageous than conventional pyrolysis because it offers time savings, increases heating efficiency, and promotes a more precise process control. In this work, the microwave-assisted pyrolysis (MAP) of brewer's spent grain (BSG), the main waste of the brewing industry, was studied, focusing on its liquid product. The effects of temperature, moisture content, and catalyst (calcium oxide) percentage on the product distribution and hydrocarbon content in the liquid product obtained were investigated. Although a high liquid yield of 71.8% was achieved with a BSG moisture content of 14%, the quality of the product (hydrocarbon yield) in this condition was not so attractive (21.60%). An optimization study was carried out to simultaneously maximize bio-oil yield and quality. The optimum conditions obtained were a temperature of 570 °C and a catalyst/biomass ratio of 12.17%. The results of the liquid product composition at the optimum point are promising given the presence of aromatic hydrocarbons, organic compounds of great interest to the industry.

Keywords: biomass; catalytic microwave-assisted pyrolysis; calcium oxide; hydrocarbons

Citation: Pimenta, F.; Filho, E.; Diniz, Â.; Barrozo, M.A.S. Catalytic Microwave-Assisted Pyrolysis of the Main Residue of the Brewing Industry. *Catalysts* **2023**, *13*, 1170. https://doi.org/10.3390/catal13081170

Academic Editors: Zixian Jia and Anton Naydenov

Received: 6 June 2023
Revised: 21 July 2023
Accepted: 26 July 2023
Published: 30 July 2023

1. Introduction

The valorization of underutilized agro-industrial wastes represents a significant opportunity in view of the growing demands for energy, the impacts of fossil fuel on the global environment, and people's concern with the improper disposal of solid wastes because of their serious impact on global warming and land use. These concerns have encouraged the development of alternative technologies to use these wastes for the generation of clean and renewable energy [1]. Pyrolysis is a thermochemical technique used to decompose biomasses into different products, such as bio-oil or other high-value chemicals, combustible gases, and biochar [2–4].

Brewer's spent grain (BSG) is the main by-product of the brewing industry, representing 85% of the total by-products generated in the brewing process [5,6]. This lignocellulosic material can be used in a thermochemical conversion process such as pyrolysis as a source of high-value products or as a petroleum fuel substitute in the long term [7–9].

The valorization of BSG was recently studied using conventional sources of heating in a fixed bed reactor to perform the slow pyrolysis, and a high liquid yield was achieved (60.7%) at 650 °C [10]. In addition, some work was also performed to study the fast pyrolysis and the fluid dynamics behavior of mixtures of sand and BSG in a spouted bed. The authors found a bio-oil rich in phenolic and nitrogenated compounds [7]. Some kinetic studies on the pyrolysis of BSG were also performed [9,11,12]. However, in these previous works of the BSG pyrolysis, the heating was performed using an electrical source, which is inefficient and energy-intensive.

Alternative heating systems for the pyrolysis process have been investigated in the last decades [13–16]. The microwave-assisted pyrolysis (MAP) process offers some advantages

over traditional pyrolysis, such as precise, controlled, and selective heating [17–21]. Despite these advantages, there are still several challenges to be overcome—for instance, the low bio-oil yield compared to that obtained in conventional configurations for some types of biomass [22]. Therefore, in order to transfer this pyrolysis technology to the industrial sector, further studies are needed to overcome this and other issues, e.g., the quality of the obtained products [23–25].

The yield and quality of the bio-oil obtained via MAP can be significantly affected by the characteristics of the raw material [26,27]. For example, although the moisture content of biomass can improve the overall efficiency of microwave radiation energy absorption [28], a very high moisture content can impair the bio-oil quality [29–31]. Most of the studies employing MAP used a biomass moisture content lower than 16% (wet base) [32–35]. Nonetheless, it is still a challenge to find the best moisture content in order to improve the yield and quality of pyrolysis products.

There is an increasing amount of research studies focused on the use of microwaves in the pyrolysis of biomass feedstocks, such as corn stover [29,36], pine sawdust [32,37–39], bamboo sawdust [39,40], oil palm male flowers [41], palm kernel shells [42], oil palm empty fruit bunches [43], rice husks [44–46], macadamia shells [47], wood [48,49], sugar cane bagasse [50,51], walnut shells [52], orange peels [53], banana peels [54], and seeds [55,56], among others. According to these publications, the use of microwave heating in the pyrolysis of biomass can enhance the production of biofuels and chemicals products. However, the results are strongly dependent on process parameters.

Some of the latest research in microwave-assisted pyrolysis has demonstrated the importance of this method to achieve the production of different products of interest, especially liquid products. One of these publications addresses the production of aviation oil using plastic waste as feedstock for the MAP. The authors point out that the liquid product obtained showed many hydrocarbons of a long chain. For polypropylene, for example, C8–C16 hydrocarbons were 91.02% of the area. This work highlights microwave-assisted pyrolysis as a method to successfully achieve the production of fuels [57]. The interest in contributing to the development of alternative sources of energy, such as biofuels, has also led to some studies using MAP of microalgae (*Chlorella vulgaris*) and low-rank coal with 1 wt.% HZSM-5 catalyst. The authors found a bio-oil yield of 33.8 wt.% in the best conditions, with a composition composed of several groups, including hydrocarbons [58]. Another publication compared pyrolysis using microwave heating and electric heating of spent bleaching clay, and the authors addressed that the microwave heating saved up to 53% of the energy consumption in the proposed comparison, resulting in high production of aromatics in the bio-oil [59]. Several studies state the strong sensitivity of the yield and quality of the microwave-assisted pyrolysis products to the operational parameters [60–65].

The effects of catalysts on thermochemical conversion processes of biomass have been the focus of many researchers [35,66–69]. Catalyst selectivity is important for optimizing the distribution of products and improve their quality. In this study, we choose calcium oxide (CaO) as the catalyst because it is a cheap catalyst when compared to zeolites and other catalysts. Additionally, a CaO catalyst has the ability to improve the composition of the liquid product, especially related to its action in the decarbonylation of ketones, which results in the formation of CO and hydrocarbons. Chen et al. [70] worked on the pyrolysis of cellulose, hemicellulose, and lignin—the main components of lignocellulose biomasses—in the presence of CaO, and they found that at temperatures ranging from 400 °C to 600 °C, the use of CaO contributed to the conversion of acids. Regarding cellulose, the CaO reduced the yield of sugars that suffer from catalytic cracking at higher temperatures. Concerning the use of CaO in the pyrolysis of lignin, the authors found that at these temperatures, phenol content decreases [70]. Thus, based on this and other results of the literature [71–76], it is expected that the addition of calcium oxide in microwave-assisted pyrolysis of BSG can produce a liquid product with low acids and phenols contents and high hydrocarbon yields.

Catalytic pyrolysis can be classified as in situ or ex situ. In the first case, the catalyst is mixed with the biomass, and in ex situ configurations, the biomass is pyrolyzed separated and the catalyst is kept in a catalyst bed [77]. The reusability of the spent catalyst is an important factor. In this work, the use of spent CaO was not performed because we used in situ configuration. However, many authors have reported these studies in pyrolysis, especially in ex situ configurations. Yi et al. [78] studied the ex situ catalytic pyrolysis of biomass (Jatropha seeds cake) in a fixed-bed reactor and compared the use of different CaO (organic and conventional). In their study, they mentioned that ex situ configuration contributes to the separation of char and CaO. Furthermore, they showed that the regeneration of the spent CaO was performed via calcination in a muffle furnace at 900 °C for 0.5 h, conditions capable of completely removing the coke deposition for the conventional CaO regenerated 10 times over. Gupta et al. [79] performed fast pyrolysis of oakwood using partially hydrated CaO, and according to them, the catalyst showed good structural stability after catalytic tests. Kumagai et al. [80] studied the pyrolysis of polyethylene terephthalate (PET) using calcium oxide. In terms of GC area percentages, they found that over 10 repetitions, the product distribution in the CaO catalysts analyzed did not show significant changes. Castello et al. [81] also reported that in catalytic pyrolysis of biomass, the in situ configuration deals with the difficulty in distinguishing the catalyst and biochar.

Despite many efforts made in many studies of the pyrolysis of different materials using different catalysts, additional studies of the catalytic microwave-assisted pyrolysis are necessary to overcome some limitations of this technique, mainly related to the product quality, which is strongly affected by moisture content, type of catalyst, and other operating parameters.

In this work, the microwave-assisted pyrolysis of BSG was investigated for the first time with the aim of improving the performance of this methodology for the valorization of this underutilized agro-industrial waste. A detailed statistical analysis was performed using regression techniques to quantify the effects of temperature (T), moisture content (MC), and calcium oxide ratio (% Cat) on the yield of the three pyrolysis products, i.e., gas, liquid, and char. An optimization study was also carried out to find the ideal conditions for a high liquid product (bio-oil) yield with a high hydrocarbon yield.

2. Results and Discussion

2.1. MAP Products Yields

The yields of the three products obtained in the first central composite design (CCD) for the MAP process of BSG are presented in Table 1.

Table 1. Product yields from the microwave-assisted pyrolysis of BSG.

Run	T (°C)	MC (%)	% Solid	% Liquid	% Gas *
1	450	5.43	34.9	48.4	16.7
2	450	12.57	23.8	66.0	10.2
3	550	5.43	43.3	35.3	21.4
4	550	12.57	17.1	70.0	12.9
5	430	9	28.6	56.9	14.5
6	570	9	17.6	42.4	40.0
7	500	3.95	46.9	38.4	14.7
8	500	14.05	11.3	71.9	16.8
9	500	9	23.5	62.0	14.5
10	500	9	26.1	64.5	9.3

* Determined by the difference based on the mass balance (wt.%).

Kinetic studies on the pyrolysis of BSG were performed previously by our research group and is reported in a related paper [9]. The highest liquid yield was 71.9 wt.%, as observed in run 8 carried out at a temperature of 500 °C and a BSG moisture content of 14%. This result is higher than most of the values reported in the literature for microwave-assisted

pyrolysis processes of various biomasses. Borges et al. [34] used samples of wood sawdust with a moisture content (MC) of 5.15% and semi-continually dropped them into the reactor, obtaining organic condensates with 65 wt.%. Huang et al. [82] studied the pyrolysis process of rice straw with an MC of 5.46% and obtained liquid production with a maximum of about 50 wt.%. Shang et al. [83] investigated the microwave-assisted pyrolysis of sawdust with an MC of 15.87% and activated carbon as additive, achieving a liquid product yield of approximately 28 wt.%. Mamaeva et al. [84] studied the catalytic microwave pyrolysis of peanut shells with an MC of 8.03 wt.% using activated carbon in a ratio of 8:1 at 500 °C and obtained a liquid yield of 16.62 wt.%.

As observed, high moisture contents of biomass, as is the case of run 8 (14%), favor the overall efficiency of microwave radiation energy absorption; thus, the bio-oil yield is significantly affected by the aqueous fractions [85]. According to some authors, the content of water in the liquid product of pyrolysis is one of the main problems to promote its use as fuel. In addition, the water content in pyrolytic liquid also impacts the storage step due to the corrosiveness and microbial activity [30,86]. Further studies are still needed to determine the entire effects of high moisture content on pyrolytic liquid product quality. Based on comparative studies with different catalysts for the fast pyrolysis of cotton stalks, Chen et al. [87] observed that CaO had the best behavior contributing to the low moisture content in the liquid product.

The liquid product obtained from the MAP of BSC in each experiment of the first CCD was analyzed by GC/MS. The detected compounds were classified into three different groups (hydrocarbons, oxygenated compounds, and nitrogenous compounds), and the respective results are listed in Table 2. The highest hydrocarbon content was obtained in run 7, which was performed at 500 °C and with the lowest moisture content (3.95%). Hydrocarbons are valuable components in bio-oil from the point of view of fuel application. Aromatic hydrocarbons serve as important industrial chemicals and fuel additives to increase the octane number [21].

Table 2. GC/MS results obtained from the microwave-assisted pyrolysis of BSG in the first CCD.

Run	T (°C)	MC (%) *	% Hydrocarbons	% Oxygenated	% Nitrogenous
1	450	5.43	22.04	58.32	11.18
2	450	12.57	14.31	45.97	7.09
3	550	5.43	35.72	48.85	9.04
4	550	12.57	17.51	58.96	11.68
5	430	9	11.83	50.6	27.5
6	570	9	32.65	41.75	14.5
7	500	3.95	48.85	51.15	0
8	500	14.05	21.6	52.95	12.96
9	500	9	29.21	45.37	13.96
10	500	9	31.58	45.96	11.17

* Moisture content of BSG (wt.%).

The experimental results of the first central composite design (Tables 1 and 2) were used to quantify the effects of the studied independent variables (T and MC) on the liquid and hydrocarbon yields using regression techniques. Table 3 shows the results of the statistical analysis with the significant values of each independent variable (T and MC), including linear, quadratic, and interaction coefficients. The analysis of the variance framework was used to determine the significance of the parameters. A factor or interaction was considered significant when the p-value satisfied the relationship $p < 0.05$ for a confidence level of 95%. Thus, factors or interactions with $p > 0.05$ were considered statistically non-significant.

Table 3. Effects of temperature and moisture content on the liquid and hydrocarbon yield.

Factor	Liquid Product (R^2 = 0.97)			Hydrocarbon Yield (R^2 = 0.89)		
	Effect	Std. Err.	*p*-Value *	Effect	Std. Err.	*p*-Value *
Mean	63.26	2.09	$<1 \times 10^{-2}$	30.39	3.91	$<1 \times 10^{-2}$
T	−3.69	1.04	0.02	5.79	1.95	0.04
T^2	−6.17	1.38	0.01	−5.66	2.59	0.09
MC	12.45	1.04	$<1 \times 10^{-2}$	−8.05	1.95	0.01
MC^2	−3.41	1.38	0.06	0.83	2.59	0.76
T.MC	4.30	1.48	0.04	−2.62	2.76	0.39

* Considering the confidence level of 95%.

Figure 1 shows the surface and contours for liquid and hydrocarbon fraction yields as functions of the independent variables (T and MC) obtained by the parameters in Table 3. As observed, the increase in temperature caused more volatile materials to be released, resulting in greater bio-oil production. Therefore, the highest liquid yield was obtained at temperatures around 500–550 °C (Figure 1a). The linear effect of MC on the bio-oil yield indicates that higher BSG moisture contents also lead to a high liquid yield. This suggests that high moisture contents in the wet biomass improve the efficiency of microwave radiation energy absorption, which in turn favors the pyrolysis process. However, the bio-oil obtained can be diluted by the aqueous fractions, which ends up affecting its quality, as seen in Figure 1b. The condition that simultaneously improved both responses (liquid and hydrocarbon yields) was a temperature around 500 °C and a low moisture content.

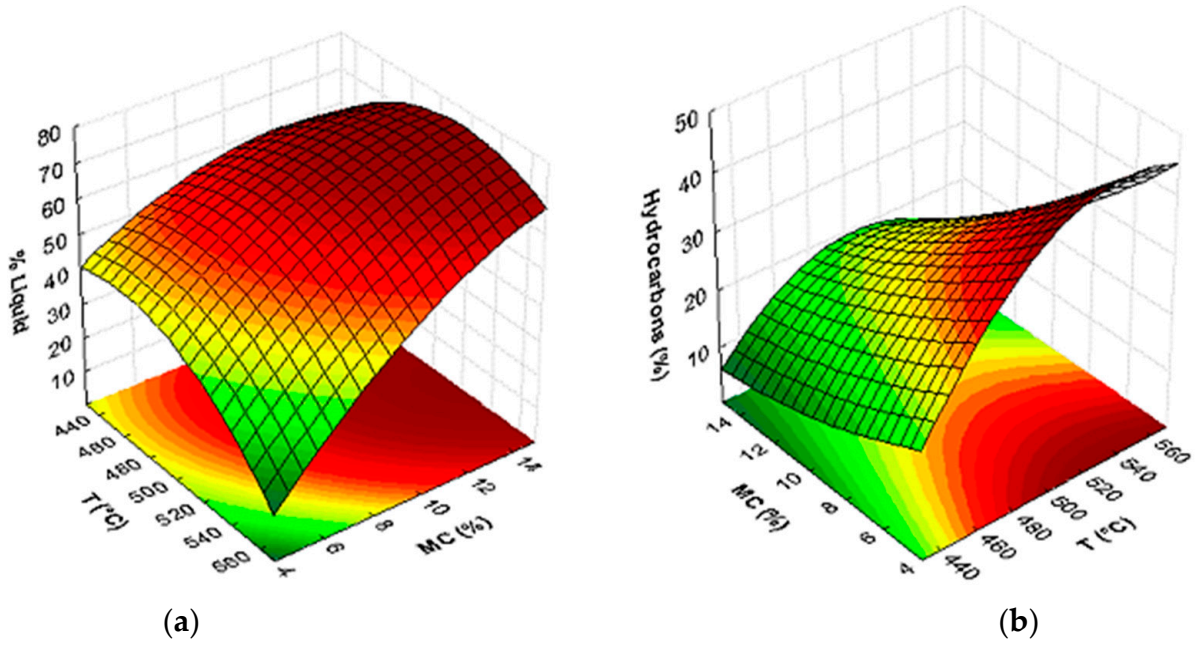

Figure 1. Response surface of liquid (**a**) and hydrocarbon (**b**) yields.

2.2. Catalyst Characterization

The results obtained from the X-ray diffraction (XRD) analysis of the catalyst (calcium oxide) used in the catalytic MAP experiments reveal characteristics of a homogeneous catalyst consisting mainly of pure CaO, calcium carbonate, and calcium hydroxide, as shown in Figure 2.

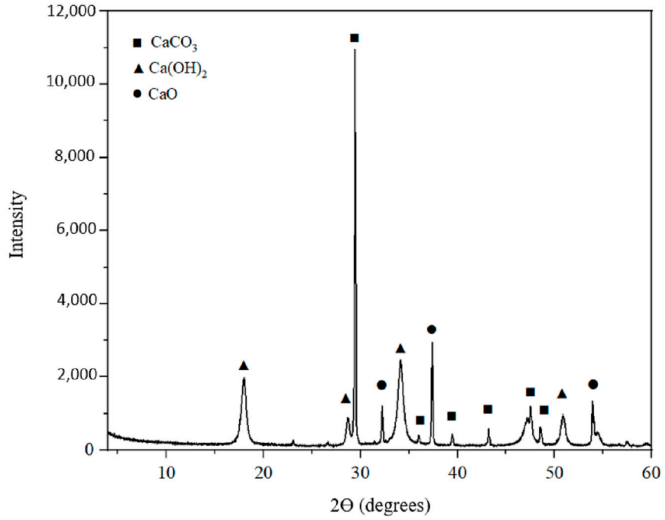

Figure 2. X-ray diffraction analysis of the catalyst.

As it can be seen in Figure 2, the XRD pattern of the catalyst exhibits a strong peak in the 2θ range of 28.5–30.0 and five small weak peaks in the 2θ range of 36.0–48.6 due to the formation of calcium carbonate. In addition, there are peaks in the 2θ range of 33.4–54.3 which are typical of pure calcium oxide. There are also characteristic peaks of calcium hydroxide that can be associated with the fact that water was absorbed from the environment [88].

The results of the thermogravimetric (TG) and differential thermogravimetric (DTG) analyses of the fresh CaO catalyst used in this work as well as the spent CaO catalyst (after run 6) are shown in Figure 3.

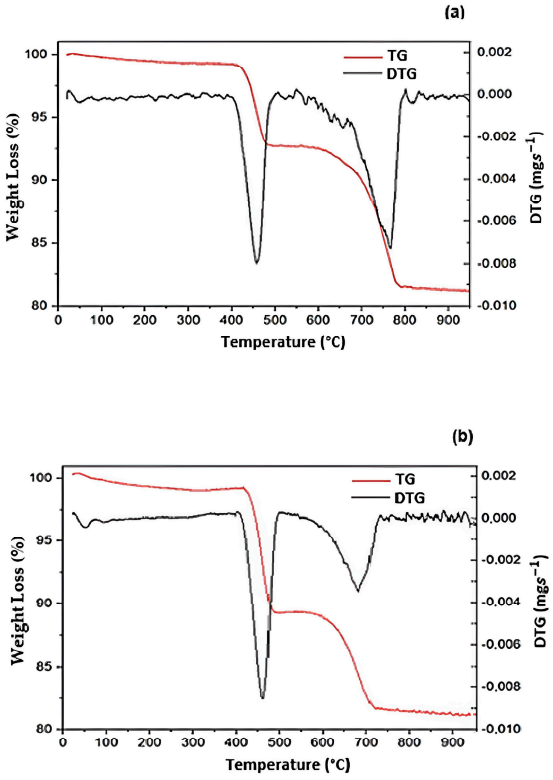

Figure 3. TG and DTG curves of CaO used as metal oxide catalyst (**a**) prior to experiments (fresh), and (**b**) after run 6 from the catalytic CCD.

According to Figure 3a, the TG/DTG curves of the fresh CaO catalyst show two events of mass losses. The first loss between 50 and 470 °C can be related to the water loss on the CaO surface kept by hydrogen bonds [89]. The water adsorption on this metal oxide happens due to the contact of CaO with moisture during exposure in the handling step [90,91]. The second mass loss occurs between approximately 650 and 762 °C and is related to the decomposition of calcium carbonate ($CaCO_3$), resulting in calcium oxide (CaO) and CO_2 formation [89]. According to Figure 3b, the TG/DTG curves of the spent CaO after run 6 (570 °C and 15 cat %) also show two weight losses. The results of the spent catalyst and the CaO prior to the experiment showed similar behavior, and as mentioned in previous works [77,78], they show good potential for reusability. Zhang et al. [92] also reported analyzes of CaO after the pyrolysis of poplar, cellulose, and lignin, and they showed that the slight difference observed in the spent catalysts was due to the coke deposits.

2.3. Catalytic Effects on the Distribution of MAP Products

The results of the products obtained from the catalytic MAP of brewer's spent grain are summarized in Table 4. As can be seen, the formation of liquid product was significantly affected by the presence of the catalyst.

Table 4. Product yields obtained from the catalytic microwave-assisted pyrolysis of BSG.

Run	T (°C)	Cat (%) *	% Solid	% Liquid	% Gas
1	450	10	37.68	29.89	32.43
2	450	20	40.65	27.72	31.63
3	550	10	30.04	31.70	38.28
4	550	20	37.70	24.90	37.40
5	430	15	45.22	28.90	25.88
6	570	15	35.35	32.82	31.83
7	500	8	31.58	33.87	34.55
8	500	22	47.85	23.86	28.29
9	500	15	40.68	19.97	39.35
10	500	15	42.40	23.34	34.26

* Catalyst/biomass ratios.

In general, the addition of the catalyst (CaO) to the microwave-assisted pyrolysis process (Table 4) resulted in a reduced bio-oil yield compared to the values obtained without the use of the catalyst at the same temperature (Table 1). The use of CaO promotes the cracking of bio-oil components, consequently increasing the gas yield. This difference is influenced by the pyrolysis temperature, since higher temperatures are more favorable to the cracking of volatiles in the presence of CaO [93–95]. However, despite the decrease in the liquid product yield, the quality of the bio-oil obtained in this study improved when the pyrolysis process was carried out in the presence of the catalyst according to the results of the GC/MS analysis (Table 5).

Table 5. GC/MS results from the catalytic microwave-assisted pyrolysis of BSG.

Run	T (°C)	Cat (%) *	% Hydrocarbons	% Oxygenated	% Nitrogenous
1	450	10	36.67	40.81	10.21
2	450	20	36.85	42.31	8.98
3	550	10	52.27	26.36	11.73
4	550	20	54.58	24.60	10.98
5	430	15	35.45	42.83	10.48
6	570	15	53.16	26.40	11.97
7	500	8	46.45	32.35	9.52
8	500	22	47.08	31.11	11.62
9	500	15	50.94	27.09	9.65
10	500	15	51.29	38.50	9.79

* Catalyst/biomass ratios.

The GC/MS analysis of the liquid product yields showed that the content of hydrocarbons present in the bio-oil drastically increased, while the content of oxygenated compounds was reduced when the catalyst (calcium oxide) was used in the MAP. As reported, the CaO can promote bio-oil deoxygenation through decarboxylation and dehydration reactions, which ends up improving its quality [73,95]. The use of CaO can also have a deacidification effect, decreasing the content of oxygenated species, such as formic acid, acetic acid, and levo-glucose during the pyrolysis of biomasses [72,96].

The yield of ketones (oxygenated compounds) decreases in the presence of CaO due to the catalytic decarbonylation of linear ketones to form carbon monoxide at high temperatures [72]. CaO also reacts with phenols, promoting the cracking of the branched chain of phenols at high temperatures to form hydrocarbons and CO [70,97]. Figure 4 shows the composition of the bio-oil obtained from MAP of BSG carried out at a temperature of 550 °C using different CaO/biomass ratios (0%, 5%, 10%, 15% and 20%). As can be seen, the increase in the catalyst ratio (Cat %) reduced the oxygenated compounds and increased the hydrocarbons present in the liquid product.

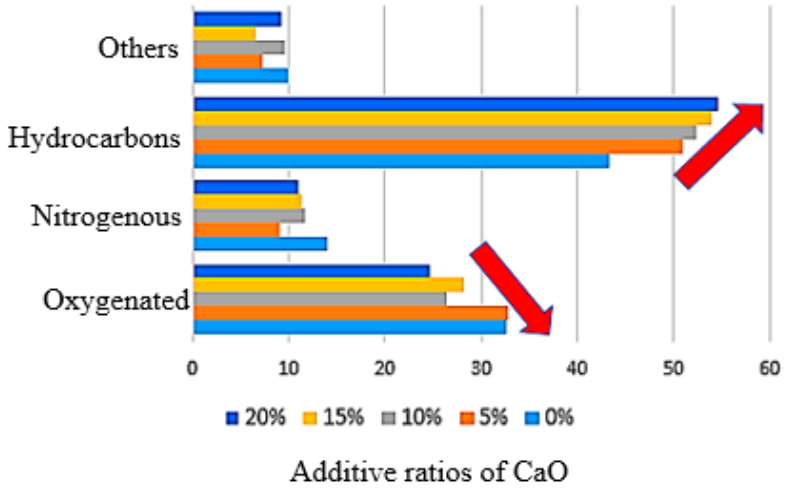

Figure 4. Catalyst effect on bio-oil quality at 550 °C (the red arrows show the behavior of hydrocarbons and oxygenated after catalytic MAP with different additive ratios of CaO).

The results of the liquid and hydrocarbon yields obtained in the experiments performed with the catalyst (Tables 4 and 5) were statistically treated using regression techniques to quantify the effects of the independent variables (T and Cat) on these responses. Table 6 shows the results of parameters related to the linear, quadratic and interaction effects of these variables, together with the respective variance analysis. The parameters with a *p*-value higher than 0.05 were considered non-significant.

Table 6. Effects of temperature and catalyst on the liquid and hydrocarbon yield.

Factor	Liquid Product (R^2 = 0.90)			Hydrocarbon Yield (R^2 = 0.98)		
	Effect	Std. Err.	*p*-Value *	Effect	Std. Err.	*p*-Value *
Mean	21.65	1.493	$<1 \times 10^{-2}$	51.11	1.08	$<1 \times 10^{-2}$
T	0.56	0.74	0.49	7.29	0.54	$<1 \times 10^{-2}$
T^2	4.27	0.98	0.01	−3.51	0.71	0.01
Cat	−2.89	0.74	0.01	0.42	0.54	0.47
Cat^2	3.27	0.98	0.03	−2.28	0.71	0.03
T.Cat	−1.15	1.05	0.33	0.53	0.76	0.52

* Considering the confidence level of 95%.

As observed, both variables (T and Cat) significantly influenced the bio-oil and hydrocarbon yields but did so in a non-linear way. This non-linear effect can be explained by

two competing factors: the higher gas residence time due to the presence of the catalyst in the bed and the occurrence of secondary thermal cracking reactions [70,96].

Figure 5 shows the response surface and the respective contours for liquid and hydrocarbon fraction yields as functions of the studied independent variables. Considering both responses simultaneously, the best conditions for the studied variables were higher temperatures (T) and intermediate catalyst ratio (Cat) values. However, to find the most precise optimum condition, it was necessary to perform an optimization study.

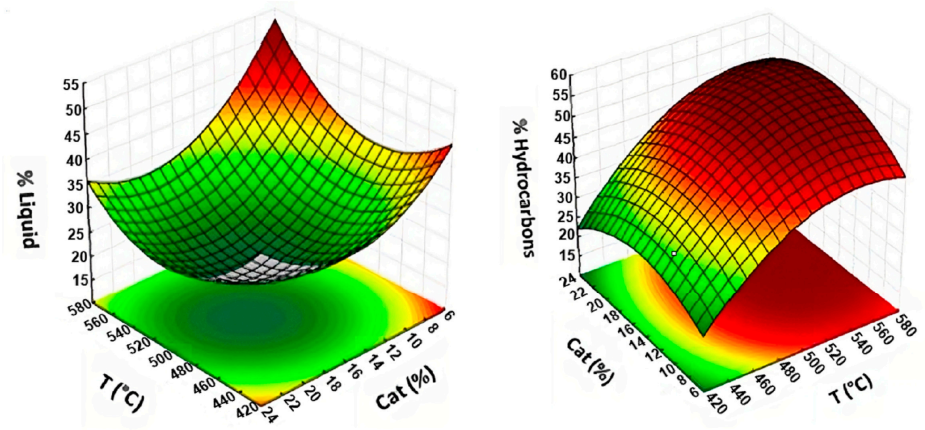

Figure 5. Response surface of liquid product and hydrocarbon yields.

2.4. Optimization Study and Analysis of Products

In this work, a multi-response optimization was performed to find the operating conditions that simultaneously maximized the bio-oil yield and its hydrocarbon content. The optimization study was carried out using the Desirability function [98]. In this technique, the composite function that combines the individual responses in the best way is named Global Desirability [99] and is commonly used in the RSM framework. The desirability values vary between 0 and 1, 0 being an undesirable response and 1 a desirable value [16].

Table 7 shows the optimization results with coded and real values of the independent variables for the optimum conditions as well as the respective values of liquid product (y_1) and hydrocarbon (y_4) yields calculated using the respective prediction equations. The optimum conditions obtained were a temperature at the highest level (570 °C) and a catalyst percentage of 12.17%. Table 7 also includes the results of a confirmatory experiment performed under these optimum conditions. The experimentally obtained hydrocarbon yield (y_4) was higher than that achieved in all runs of the central composite design (CCD) (Table 5) and in most of the results reported in the literature for biomass pyrolysis [29,33,84]. This result confirms the high quality of the bio-oil obtained from the MAP under these optimum conditions.

Table 7. Optimization results: predicted and experimental data from the simultaneous maximization of liquid and hydrocarbon yields.

Coded Variable	Original Form	Coded Values	Uncoded Values
x_2	*T* (°C)	1.414	570 °C
x_3	*Cat* (%)	−0.565	12.17%
Yield (%)	**Predicted Value**	**Experimental Data ***	
y_1**(Liquid)**	32.87	30.88	
y_4**(Hydrocarbons)**	53.67	61.58	

* Experiment performed under these optimum conditions.

The liquid product obtained in the experiment carried out under the optimum conditions (a temperature of 570 °C and a catalyst percentage of 12.17%) was analyzed by GC/MS. Table 8 lists the main compounds found.

Table 8. Compounds in the bio-oil produced in the MAP optimization experiment.

RT (min)	Compound *	Formula	% Area
25.318	Undecane	$C_{11}H_{24}$	0.76
11.279	Toluene	C_7H_8	6.28
18.124	Styrene	C_8H_8	4.61
61.528	Phenanthrene	$C_{14}H_{10}$	1.11
17.639	Orthoxylene	$C_8\ H_{10}$	2.06
14.899	Nonane	C_9H_{20}	0.43
40.262	Isopropylmethylnaphthalene	$C_{14}H_{16}$	4.84
26.972	Indene	C_9H_8	4.35
39.589	Hexadecane	$C_{16}H_{34}$	5.59
15.706	Ethylbenzene	C_8H_{10}	1.74
30.345	Dodecane	$C_{12}H_{26}$	0.67
20.087	Decano	$C_{10}H_{22}$	0.66
42.442	Cyclopropylphenylmethane	$C_{10}H_{12}$	0.54
48.224	Biphenylene	$(C_6H_4)_2$	2.04
46.711	Biphenyl	$C_{12}H_{10}$	0.74
20.499	Propylbenzene	C_9H_{12}	0.55
31.043	Pentylbenzene	$C_{11}H_{16}$	0.78
35.945	Hexylbenzene	$C_{12}H_{18}$	0.62
25.935	butylbenzene	$C_{10}H_{14}$	0.46
23.570	2-Propenylbenzene	C_9H_{10}	0.81
22.179	1-Ethyl-2-Methylbenzene	C_9H_{12}	0.53
23.685	1-Methyl-3-Vinylbenzene	C_9H_{10}	0.91
16.144	1.3-Dimethylbenzene	C_8H_{10}	1.97
36,475	1,3-Dimethylbutylbenzene	$C_{12}H_{18}$	0.52
35.115	Azulene	$C_{10}H_8$	8.98
47.979	3-Octadecene	$C_{18}H_{36}$	0.39
25.445	1-Undecene	$C_{11}H_{22}$	1.46
35.245	1-Tridecene	$C_{13}H_{26}$	3.22
14.997	1-Noneno	C_9H_{18}	0.54
32.131	1-Methylindene	$C_{10}H_{10}$	1.25
30.477	1-Dodecene	$C_{12}H_{24}$	1.35
20.196	1-Decene	$C_{10}H_{20}$	0.82
	Hydrocarbons		61.58
16.033	Pyrrole	C_4H_5N	1.95
27.497	Benzonitrile	C_6H_5CN	1.35
37.143	Benzyl cyanide	$C_6H_5CH_2CN$	0.8
39.209	Isoquinoline	C_9H_7N	0.91
46.244	Indole	C_8H_7N	3.1
49.338	1H-Indole, 3-methyl-	C_9H_9N	0.38
64.417	Hexadecanenitrile	$C_{16}H_{31}N$	1.16
78.132	Octadecanamide	$C_{18}H_{37}NO$	1.07
	Nitrogenated		10.72
31.642	Phenol	C_6H_6O	3.88
33.955	Phenol, 2-methyl-	C_7H_8O	3.75
35.679	Phenol, 4-methyl-	C_7H_8O	4.75
37.857	Phenol, 2,3-dimethyl-	$C_8H_{10}O$	1.37
43.689	2-Methoxy-4-vinylphenol	$C_9H_{10}O_2$	3.06
	Phenols		16.81
29.886	2-Cyclopenten-1-one,2,3-imethyl-	$C_7H_{10}O$	0.76
62.525	2-Nonadecanone ketones	$C_{19}H_{38}O$	3.05
	Ketones		3.81
39.748	2-Nonenal	$C_9H_{16}O$	3.75
	Aldehydes		3.73

* Main compounds found in the experiment performed under optimum conditions.

According to Table 8, the bio-oil produced has a diverse composition, in which the high content of hydrocarbon compounds (61.58%) stands out. Although substantial amounts of hydrocarbons are desirable for their use as fuel oil, this liquid product from the catalytic

MAP can also be a source of value-added chemicals and therefore a supply of intermediary chemical species, such as phenolic compounds and aromatic hydrocarbons, among others. Phenolic compounds are also used in the food industry as flavorings, in the manufacture of adhesives and polymers, and as intermediates in pharmaceutical syntheses [9,29,100–103]. In addition, as reported by other authors, CaO was effective in removing acids with high oxygen content [95]. A low % area related to the acids was also found in all the experimental runs of the catalytic MAP of BSG (see Supplementary Material).

Some experiments of the CCD of the catalytic MAP were selected to analyze the physicochemical properties (water content and viscosity) of the liquid product generated. The results obtained are presented in Table 9.

Table 9. Physicochemical properties of the liquid product of some tests of the catalytic MAP of BSG.

Physicochemical Properties of the Liquid Product				
Run	**T(°C)**	**Cat (%)**	**Water Content (%)**	**Viscosity (Pa.s)**
5	430	15	23.85 ± 2.03	$0.01 \pm 4.43 \times 10^{-4}$
6	570	15	40.36 ± 2.22	$0.01 \pm 1.13 \times 10^{-4}$
7	500	8	49.54 ± 1.75	$0.02 \pm 1.78 \times 10^{-4}$
8	500	22	20.04 ± 1.36	$0.01 \pm 1.94 \times 10^{-4}$
10	500	15	66.41 ± 3.70	$0.02 \pm 2.16 \times 10^{-5}$

It can be seen that the lowest water content in the liquid product was obtained in the experiment carried out with the highest catalyst loading (22%), evidencing the good performance of the CaO catalyst in reducing the water content of the bio-oil. Similar behavior for the water content in the liquid product was found in a study about the catalytic MAP of corn stover [29].

2.5. Solid Product Characterization

Scanning electron microscopy (SEM) analysis was used to analyze the morphological changes caused by the thermal degradation of brewer's spent grain. Figure 6 shows SEM photomicrographs of the BSG at 50 and 200× magnification and of the solid product obtained from the microwave-assisted pyrolysis carried out under optimized conditions (temperature equal to 570 °C and 12.17% catalyst ratio). The surface of the solid product from the MAP optimization experiment is not homogeneous, with fibrous texture regions due to the influence of the thermal degradation of the biomass [10].

Figure 6. SEM micrographs of brewer's spent grain (BSG) above and the solid products obtained under optimized conditions at 50 and 200× magnification.

2.6. Catalyst Action

Calcium oxide is known to show significant deoxygenation activity when used in the pyrolysis of biomass [104]. Wang et al. [75] studied the pyrolysis of corncob using CaO as catalyst. They explained that the reduction in the number of acids generated as a product can also be related to the neutralization reaction, which originates calcium carboxylate and water. In addition, the authors also mention that some reactions involving CaO and phenols can be responsible for the formation of hydrocarbons at low temperatures [75]. Chen et al. [95] reported in their publication that, the calcium carboxylate is decomposed to $CaCO_3$ and ketones. According to Li et al. [72] the deoxygenation reaction of oxygenated compounds with calcium oxide catalyst can be represented by three pathways: neutralization (represented by Equations (1) and (2), thermal cracking (represented by Equation (3)), and catalytic cracking (Equation (4)), as shown below [75,105,106]:

$$CaO + 2R - COOH \rightarrow (R - COO)_2Ca + H_2O \quad (1)$$

$$(R - COO)_2Ca \rightarrow CaCO_3 + R - COR \quad (2)$$

$$R - COOH \overset{CaO}{\rightarrow} CO_2 + RH \quad (3)$$

$$CaO + R - COOH \rightarrow CaCO_3 + RH \quad (4)$$

Neutralization reactions take place at a lower temperature, while thermal cracking and catalytic cracking reactions occur at higher temperature [74,107]. Thus, the increase in water content at lower pyrolysis temperatures may be associated with the deoxygenation mechanism [108].

Chen et al. [70] demonstrated that the use of CaO in the pyrolysis of hemicellulose, cellulose, and lignin generates lower amounts of pyrolitic compounds. The authors also mentioned that the CaO could be related to the formation of CO due to the decarbonylation of ketones (linear). In addition, these authors also explain with which compound of the biomass the CaO would react. According to them, the CaO would react with acids/esters and phenols (from hemicellulose). In cellulose, the reaction would be at a low temperature and involve the anhydrosugars, and for lignin, the reaction would occur with the phenols. The effect of the temperature was also analyzed by these authors, and they reported that at high temperatures, to form ketones/furans, the dehydration and ring-opening reaction occurs [70].

Based on experimental evidence, Case et al. [104] proposed that for the pyrolysis of cellulose, one of the proposed pathways is based on the dehydration of sugar intermediates. The authors mention that as a result, it will contribute to the formation of double bonds, that can further follow some radical addition reactions, originating dimethyl- and trimethyl-cyclopentenones [104]. In the analysis of the liquid product generated through the catalytic MAP of BSG using CaO performed in the present study, we found these same compounds.

3. Materials and Methods

3.1. Raw Material

The BSG used in this work was supplied by Abadiana Microbrewery (Minas Gerais, Brazil), which uses 100% malted barley (without the addition of other adjunct materials). The main characteristics of dried BSG are summarized in Table 10.

Table 10. Characteristics of brewer's spent grain (BSG).

Proximate Analysis (wt.%)	
HHV (MJ/kg) *	17.94 ± 3.74
Moisture	3.7 ± 0.35
Volatile matter	82.25 ± 0.03
Ash	3.19 ± 0.07
Fixed carbon	14.55 ± 0.03
Ultimate Analysis (wt.%)	
C	47.2 ± 1.3
H	7.2 ± 0.1
N	3.6 ± 0.4
S	1.1 ± 0.1
O	37.6 ± 1.7
Chemical Composition (wt.%)	
Extractives	5.26 ± 0.06
Lignin	29.37 ± 4.03
Cellulose	15.14 ± 0.03
Hemicellulose	50.23 ± 0.03

* HHV is the higher heating value.

The chemical composition of BSG was determined using a Perkin Elmer 2400 CHNS/O elemental analyzer operating at 1198 K in an atmosphere of pure oxygen. The oxygen content was calculated by difference considering the C, H, and S wt.% and the ash content. The contents of cellulose, hemicellulose, lignin, and extractives were found following the description used in our previous work [109]. Soxhlet extraction with acetone was used to estimate the extractive content. The lignin content was determined according to modified TAPPI standard T222 om-22 (2002c). Hemicellulose and α-cellulose constitute the holocellulose content, which was measured using glacial acetic acid and sodium hypochlorite at 348 ± 2 K. The α-cellulose was determined by treating the holocellulose sample with potassium hydroxide solutions of 5 and 24% (*w*/*w*). The hemicellulose content was calculated subtracting the α-cellulose content from the holocellulose [109].

The BSG showed a high H/C ratio (0.15) and an O/C ratio of 0.80. Thus, BSG has good thermal properties compared to other waste biomass materials, since for pinewood sawdust, the H/C ratio is 0.12, and for wheat stalk, it is 0.14 [110]. For wood sawdust and corn stover, the H/C ratios are both 0.12 [34]. The high quantities of carbon (47.2 ± 1.3 wt.%) are related to the energy value of a fuel because of the energy present in C-C bonds [1]. Furthermore, BSG showed high hemicellulose content compared to other major subcomponents, which offers significant potential for interesting pyrolysis products.

3.2. Microwave-Assisted Pyrolysis

The MAP experiments were carried out in a Menumaster microwave oven (model MCS10TSB, Middleby Brazil, SP, BR) at a maximum incident power of 1500 W and a frequency of 2450 MHz. The schematic diagram of the experimental apparatus is illustrated in Figure 7.

The experimental apparatus consisted of (1) gas sampling—nitrogen, (2) a heating source, (3) a PID temperature controller, (4) a quartz reactor, (5) a microwave oven, (6) a K-type thermocouple, (7) condensers, (8) a thermostatic bath, and (9) a vacuum pump.

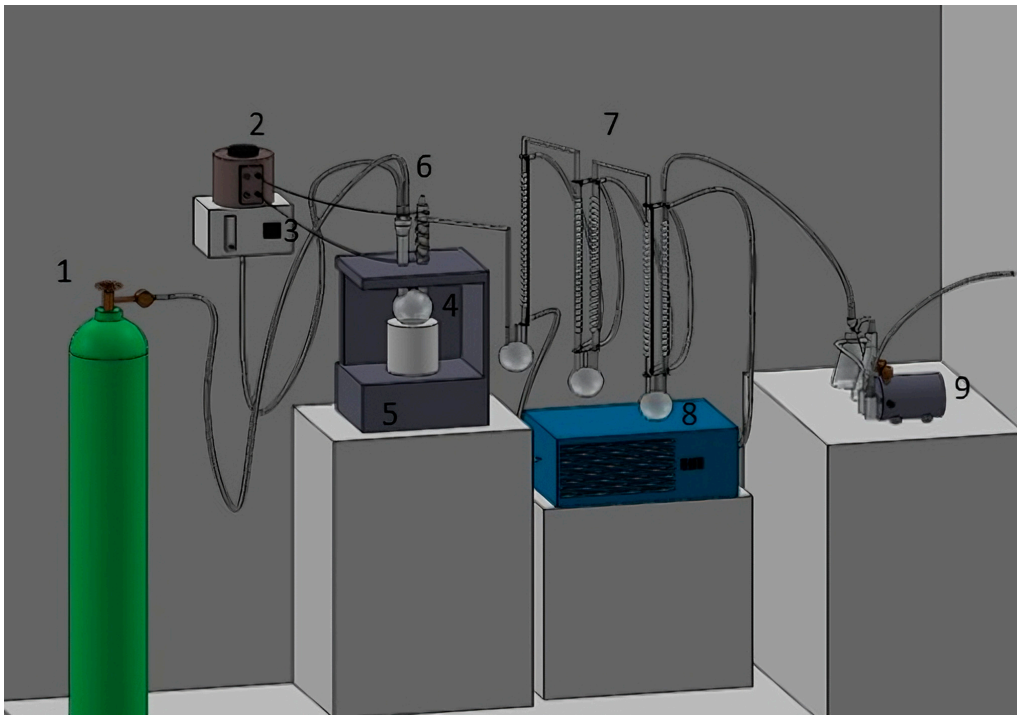

Figure 7. Schematic diagram of the MAP system: (1) gas sampling—nitrogen, (2) heating source, (3) PID controller, (4) quartz reactor, (5) microwave oven, (6) K-type thermocouple, (7) condensers, (8) thermostatic bath, and (9) vacuum pump.

Firstly, to determine the influence of moisture content on the results of the microwave-assisted pyrolysis of BSG, 70 g of biomass with different moisture contents was used. After sample preparation, the biomass was placed in the quartz reactor, which was then subjected to microwave radiation using nitrogen as an inert carrier gas at a flow rate of 50 mL/min. In order to maintain an inert atmosphere within the quartz reactor during pyrolysis, the system was vacuumed at 80 mmHg. The experiments were carried out for 30 min. The condensable components (liquid product) were collected in the condensers, while the solid residue in the reactor after pyrolysis was collected as bio-char. The yields of liquid and solid products were calculated on the basis of their actual weight, whilst the gas yield was determined by the difference based on the mass balance, as indicated in Equations (5)–(7):

$$\% \text{ Liquid} = \frac{\textit{Liquid Weight}}{\textit{Biomass Weight}} \times 100 \quad (5)$$

$$\% \text{ Solid} = \frac{\textit{Solid Weight}}{\textit{Biomass Weight}} \times 100 \quad (6)$$

$$\% \text{ Gas} = 100 - (\% \text{ Liquid} + \% \text{ Solid}) \quad (7)$$

After the identification of the moisture content of BSG that favored the bio-oil and hydrocarbon yields, a central composite design (CCD) for in situ catalytic pyrolysis was proposed, varying the percentage of catalyst (CaO) and temperature. The same previous conditions of vacuum and inert gas flow were used in these new experiments, in which 70 g of BSG (with the best moisture content identified in the first step) was initially mixed with the corresponding amount of the catalyst until the creation of a homogeneous mixture and then inserted into the reactor.

3.3. Experimental Design

In a first step, a central composite design (CCD) with 2 repetitions at the central point was used to estimate the effects of moisture content (x_1 in coded values) and temperature (x_2 in coded values) on the products of MAP of BSG. The dependent output variables were the yields of bio-oil (y_1, %), gas fraction (y_2, %), and biochar (y_3, %) as well as the yield of hydrocarbons present in the bio-oil (y_4, %). Table 11 lists the coded (x_i) and real values (moisture in % wb and T in °C) of the independent variables. The experimental results were treated using regression techniques. The software Statistica 7.0 was used to analyze the experimental data statistically. The analysis of variance (ANOVA) framework was used to determine the significance of the parameters. A confidence level of 95% was used. The central composite design (CCD), analyzed through this software, is a useful tool to determine the effect of each variable and its interactions. The use of variables in coded levels is an important way that enables the determination of the relative impact of each variable on responses (at the same level range). This helps in the comparison of the intensity of these effects on the desired responses. The coded levels are $-\alpha$, -1, 0, $+1$, and $+\alpha$, in which α is the axial point of 1.414, according to the orthogonal design [16]. The CCD was coupled with response surface methodology (RSM). The RSM technique creates a relationship between the responses and control variables [111].

Table 11. Coded and real values of the independent variables in the first central composite design.

Variables	**Levels ***				
Coded values (x_1 and x_2)	−1.414	−1	0	+1	+1.414
Moisture content (% wb)	3.95	5.43	9	12.57	14.05
Temperature (°C)	430	450	500	550	570

* Determined for the central composite design (CCD).

A second central composite design (CCD) with 2 repetitions at the central point was used to estimate the effects of catalyst/biomass ratios ($x_3$in coded values) and temperature (x_2 in coded values) on the results of the catalytic microwave-assisted pyrolysis of BSG in an in situ configuration. The dependent output variables were the yields of bio-oil (y_1, %), gas fraction (y_2, %), and biochar (y_3, %) as well as the yield of hydrocarbons present in the bio-oil (y_4, %). Table 12 presents the coded and real values of the independent variables.

Table 12. Coded and real values of the independent variables in the second central composite design for the catalytic MAP of BSG.

Variables	**Levels**				
Coded values (x_3 and x_2)	−1.414	−1	0	+1	+1.414
Catalyst (% *Cat*) *	8	10	15	20	22
Temperature (°C)	430	450	500	550	570

* Catalyst/biomass ratios.

3.4. Analysis of Products

The chemical compounds of bio-oil were characterized using the methodology described in our previous work [10]. In broad terms, gas chromatography and mass spectrometry were performed using a Shimadzu device (GC/MS-QP2010 Plus, Japan) with a an Rtx-1701 column (60 m × 0.25 mm × 0.25 µm) and helium as a carrier gas. Initially, the GC oven maintained a temperature of 45 °C for 4 min. Then, it reached 270 °C at a rate of 3 °C/min and maintained this temperature for 13 min. The temperature of the injector was 250 °C, and the split ratio was set to 100:1. The MS in electronic impact mode (EI) was operated at a mass range (m/z) of 30–300. The ion source and interface temperatures were maintained at 235 °C for a total run time of 92 min. The data of the main peaks were obtained using retention time (RT) information from the NIST library (version 08). The compounds with a similarity index higher than 80% were identified.

Bio-oil viscosity was measured following ASTM D445 standards using an R/S Plus Rheometer (Brookfield, WI, USA) with an RC3-50-1 spindle at a shear rate of 0–700 s^{-1}, shear stress of 0–601,603 mPa, time of 200 s, and a temperature of 40 °C. The water content of the bottom phase of the liquid product from the catalytic MAP was determined on a Karl Fischer titrator (Methrom 870 KF Titrino Plus, Germany). Samples of 0.2 g were used for each determination. The measurements were performed in triplicate and the results were expressed as an average.

The surface morphologies of the BSG and the biochar produced in the MAP optimization experiment were analyzed using a ZEISS EVO MA10 scanning microscope. The SEM photographs were captured at 50 and 200× magnification using an electron acceleration voltage of 5.00 kV. The samples were prepared on carbon tabs in an inert environment and coated with gold via sputter coating.

3.5. Catalyst Analysis

The catalyst used in this work was calcium oxide (CaO) (p.a.) in powder form (chemical grade, CAS: 1305-78-8), was purchased from Dinâmica Química Contemporânea LTDA, Indaiatuba, Brazil. This metal oxide was used without any further purification. The XRD analysis of calcium oxide was performed on a SHIMADZU diffractometer (model LABX XRD-6000, Japan). The XRD results were generated in a 2θ interval from 10 to 80° at a step of 0.02° and a scan rate of 2 s per step. The measurements were made using a nickel filter at a voltage of 30 kV and a current of 30 mA.

The thermogravimetric (TG) and differential thermogravimetric (DTG) analyses of the CaO used in this work were obtained using a Shimadzu TGA/DTA analyzer (DTG-60H). The purge gas used was nitrogen at a flow rate of 50 mL min^{-1}. The experiments were performed with 8 mg of sample from 303 to 1073 K at a heating rate of 5 K min^{-1}. The data were recorded using TG software to yield the mass loss (TG) and differential mass loss (DTG) curves.

4. Conclusions

In this work, the microwave-assisted pyrolysis (MAP) of brewer's spent grain (BSG), the main waste of the brewing industry, was investigated with the aim of obtaining a liquid product with a high yield and quality.

A high bio-oil yield of 71.8% was obtained with a BSG moisture content of 14%; however, the quality of this product was not so attractive (hydrocarbon yield of 21.60%). In order to improve the bio-oil quality, a catalyst (calcium oxide) was used in the pyrolysis process.

An optimization study was successfully performed, aiming at the simultaneous maximization of the bio-oil yield and quality (hydrocarbon content). The optimum conditions obtained were a temperature at the highest level (570 °C) and a catalyst percentage of 12.17%. The results of the composition of the liquid product under this optimum point using a BSG moisture content of 4% pointed to a liquid yield of 30.88% with a hydrocarbon content of 61.58%. Therefore, it can be concluded that the catalytic MAP process has an enormous potential to transform agro-industrial wastes into high-value products.

Supplementary Materials: The following supporting information can be downloaded at: https://www.mdpi.com/article/10.3390/catal13081170/s1, Table S1: % Area from GC/MS results for the liquid product from the CCD runs of the catalytic MAP.

Author Contributions: Conceptualization, F.P. and M.A.S.B.; methodology, F.P. and M.A.S.B.; software, F.P. and M.A.S.B.; validation, M.A.S.B.; formal analysis, F.P. and M.A.S.B.; investigation, F.P., E.F. and Â.D.; resources, M.A.S.B.; writing—original draft preparation, F.P.; writing—review and editing, M.A.S.B.; supervision, M.A.S.B.; project administration, M.A.S.B.; funding acquisition, M.A.S.B. All authors have read and agreed to the published version of the manuscript.

Funding: This research was funded by CAPES, CNPq, and FAPEMIG.

Data Availability Statement: The data that support the findings of this study are available from the corresponding author upon reasonable request.

Acknowledgments: The authors are grateful to CAPES, CNPq and, FAPEMIG for their financial support.

Conflicts of Interest: The authors declare no conflict of interest.

References

1. McKendry, P. Energy production from biomass (Part 1): Overview of biomass. *Bioresour. Technol.* **2002**, *83*, 37–46. [CrossRef] [PubMed]
2. Li, P.; Wan, K.; Chen, H.; Zheng, F.; Zhang, Z.; Niu, B.; Zhang, Y.; Long, D. Value-Added Products from Catalytic Pyrolysis of Lignocellulosic Biomass and Waste Plastics over Biochar-Based Catalyst: A State-of-the-Art Review. *Catalysts* **2022**, *12*, 1067. [CrossRef]
3. Wang, W.; Gu, Y.; Zhou, C.; Hu, C. Current Challenges and Perspectives for the Catalytic Pyrolysis of Lignocellulosic Biomass to High-Value Products. *Catalysts* **2022**, *12*, 1524. [CrossRef]
4. Dhyani, V.; Bhaskar, T. A comprehensive review on the pyrolysis of lignocellulosic biomass. *Renew. Energy* **2018**, *129*, 695–716. [CrossRef]
5. Mussatto, S.I.; Dragone, G.; Roberto, I.C. Brewers' spent grain: Generation, characteristics and potential applications. *J. Cereal Sci.* **2006**, *43*, 1–14. [CrossRef]
6. Reinold, M.R. *Manual Prático de Cervejaria*; Elsevier Brasil: São Paulo, Brazil, 1997.
7. Barrozo, M.A.S.; Borel, L.D.M.S.; Lira, T.S.; Ataíde, C.H. Fluid dynamics analysis and pyrolysis of brewer's spent grain in a spouted bed reactor. *Particuology* **2019**, *42*, 199–207. [CrossRef]
8. Mahmood, A.S.N.; Brammer, J.G.; Hornung, A.; Steele, A.; Poulston, S. The intermediate pyrolysis and catalytic steam reforming of Brewers spent grain. *J. Anal. Appl. Pyrolysis* **2013**, *103*, 328–342. [CrossRef]
9. Borel, L.D.M.S.; Lira, T.S.; Ribeiro, J.A.; Ataíde, C.H.; Barrozo, M.A.S. Pyrolysis of brewer's spent grain: Kinetic study and products identification. *Ind. Crops Prod.* **2018**, *121*, 388–395. [CrossRef]
10. Borel, L.D.M.S.; Reis Filho, A.M.; Xavier, T.P.; Lira, T.S.; Barrozo, M.A.S. An investigation on the pyrolysis of the main residue of the brewing industry. *Biomass Bioenergy* **2020**, *140*, 105698. [CrossRef]
11. Bieniek, A.; Reinmoller, M.; Kuster, F.; Grabner, M.; Jerzak, W.; Magdziarz, A. Investigation and modelling of the pyrolysis kinetics of industrial biomass wastes. *J Environ. Manag.* **2022**, *319*, 115707. [CrossRef] [PubMed]
12. Olszewski, M.P.; Arauzo, P.J.; Maziarka, P.A.; Ronsse, F.; Kruse, A. Pyrolysis Kinetics of Hydrochars Produced from Brewer's Spent Grains. *Catalysts* **2019**, *9*, 625. [CrossRef]
13. Martins, M.P.B.; Hori, C.E.; Barrozo, M.A.S.; Vieira, L.G.M. Solar Pyrolysis of Spirulina platensis Assisted by Fresnel Lens Using Hydrocalumite-Type Precursors. *Energies* **2022**, *15*, 7590. [CrossRef]
14. Andrade, L.A.; Barrozo, M.A.S.; Vieira, L.G.M. Catalytic solar pyrolysis of microalgae Chlamydomonas reinhardtii. *Sol. Energy* **2018**, *173*, 928–938. [CrossRef]
15. Barbosa, J.M.; Andrade, L.A.; Vieira, L.G.M.; Barrozo, M.A.S. Multi-response optimization of bio-oil production from catalytic solar pyrolysis of Spirulina platensis. *J. Energy Inst.* **2020**, *93*, 1313–1323. [CrossRef]
16. Barbosa, J.M.; Rossi, R.A.S.; Andrade, L.A.; Barrozo, M.A.S.; Vieira, L.G.M. A study of optimization of solar pyrolysis and catalyst recovery and reuse. *Energy Convers. Manag.* **2021**, *237*, 114094. [CrossRef]
17. Mushtaq, F.; Mat, R.; Ani, F.N. A review on microwave assisted pyrolysis of coal and biomass for fuel production. *Renew. Sustain. Energy Rev.* **2014**, *39*, 555–574. [CrossRef]
18. Belanger, J.M.; Pare, J.R. Applications of microwave-assisted processes (MAP) to environmental analysis. *Anal. Bioanal. Chem.* **2006**, *386*, 1049–1058. [CrossRef]
19. Motasemi, F.; Afzal, M.T. A review on the microwave-assisted pyrolysis technique. *Renew. Sustain. Energy Rev.* **2013**, *28*, 317–330. [CrossRef]
20. Chen, P.; Xie, Q.; Addy, M.; Zhou, W.; Liu, Y.; Wang, Y.; Cheng, Y.; Li, K.; Ruan, R. Utilization of municipal solid and liquid wastes for bioenergy and bioproducts production. *Bioresour. Technol.* **2016**, *215*, 163–172. [CrossRef]
21. Du, Z.; Li, Y.; Wang, X.; Wan, Y.; Chen, Q.; Wang, C.; Lin, X.; Liu, Y.; Chen, P.; Ruan, R. Microwave-assisted pyrolysis of microalgae for biofuel production. *Bioresour. Technol.* **2011**, *102*, 4890–4896. [CrossRef]
22. Domínguez, A.; Menéndez, J.A.; Fernández, Y.; Pis, J.J.; Nabais, J.M.V.; Carrott, P.J.M.; Carrott, M.M.L.R. Conventional and microwave induced pyrolysis of coffee hulls for the production of a hydrogen rich fuel gas. *J. Anal. Appl. Pyrolysis* **2007**, *79*, 128–135. [CrossRef]
23. Amalina, F.; Krishnan, S.; Zularisam, A.W.; Nasrullah, M. Effect of process parameters on bio-oil yield from lignocellulosic biomass through microwave-assisted pyrolysis technology for sustainable energy resources: Current status. *J. Anal. Appl. Pyrolysis* **2023**, *171*, 105958. [CrossRef]
24. Sharifzadeh, M.; Sadeqzadeh, M.; Guo, M.; Borhani, T.N.; Murthy Konda, N.V.S.N.; Garcia, M.C.; Wang, L.; Hallett, J.; Shah, N. The multi-scale challenges of biomass fast pyrolysis and bio-oil upgrading: Review of the state of art and future research directions. *Prog. Energy Combust. Sci.* **2019**, *71*, 1–80. [CrossRef]
25. Bridgwater, A.V. Review of fast pyrolysis of biomass and product upgrading. *Biomass Bioenergy* **2012**, *38*, 68–94. [CrossRef]
26. Mutsengerere, S.; Chihobo, C.H.; Musademba, D.; Nhapi, I. A review of operating parameters affecting bio-oil yield in microwave pyrolysis of lignocellulosic biomass. *Renew. Sustain. Energy Rev.* **2019**, *104*, 328–336. [CrossRef]
27. Wahi, R.; Zuhaidi, N.F.; Yusof, Y.; Jamel, J.; Kanakaraju, D.; Ngaini, Z. Chemically treated microwave-derived biochar: An overview. *Biomass Bioenergy* **2017**, *107*, 411–421. [CrossRef]

28. Li, J.; Dai, J.; Liu, G.; Zhang, H.; Gao, Z.; Fu, J.; He, Y.; Huang, Y. Biochar from microwave pyrolysis of biomass: A review. *Biomass Bioenergy* **2016**, *94*, 228–244. [CrossRef]
29. Mahmoud Fodah, A.E.; Ghosal, M.K.; Behera, D. Bio-oil and biochar from microwave-assisted catalytic pyrolysis of corn stover using sodium carbonate catalyst. *J. Energy Inst.* **2021**, *94*, 242–251. [CrossRef]
30. Biradar, C.H.; Subramanian, K.A.; Dastidar, M.G. Production and fuel quality upgradation of pyrolytic bio-oil from Jatropha Curcas de-oiled seed cake. *Fuel* **2014**, *119*, 81–89. [CrossRef]
31. Cornelissen, T.; Yperman, J.; Reggers, G.; Schreurs, S.; Carleer, R. Flash co-pyrolysis of biomass with polylactic acid. Part 1: Influence on bio-oil yield and heating value. *Fuel* **2008**, *87*, 1031–1041. [CrossRef]
32. Khelfa, A.; Rodrigues, F.A.; Koubaa, M.; Vorobiev, E. Microwave-Assisted Pyrolysis of Pine Wood Sawdust Mixed with Activated Carbon for Bio-Oil and Bio-Char Production. *Processes* **2020**, *8*, 1437. [CrossRef]
33. Xue, Z.; Zhong, Z.; Zhang, B. Microwave-Assisted Catalytic Fast Pyrolysis of Biomass for Hydrocarbon Production with Physically Mixed MCM-41 and ZSM-5. *Catalysts* **2020**, *10*, 685. [CrossRef]
34. Borges, F.C.; Du, Z.; Xie, Q.; Trierweiler, J.O.; Cheng, Y.; Wan, Y.; Liu, Y.; Zhu, R.; Lin, X.; Chen, P.; et al. Fast microwave assisted pyrolysis of biomass using microwave absorbent. *Bioresour. Technol.* **2014**, *156*, 267–274. [CrossRef] [PubMed]
35. Wan, Y.; Chen, P.; Zhang, B.; Yang, C.; Liu, Y.; Lin, X.; Ruan, R. Microwave-assisted pyrolysis of biomass: Catalysts to improve product selectivity. *J. Anal. Appl. Pyrolysis* **2009**, *86*, 161–167. [CrossRef]
36. Fodah, A.E.M.; Ghosal, M.K.; Behera, D. Quality assessment of bio-oil and biochar from microwave-assisted pyrolysis of corn stover using different adsorbents. *J. Energy Inst.* **2021**, *98*, 63–76. [CrossRef]
37. Liang, J.; Xu, X.; Yu, Z.; Chen, L.; Liao, Y.; Ma, X. Effects of microwave pretreatment on catalytic fast pyrolysis of pine sawdust. *Bioresour. Technol.* **2019**, *293*, 122080. [CrossRef]
38. Guo, F.; Qiao, Q.; Mao, S.; Bai, J.; Dong, K.; Shu, R.; Xu, L.; Wei, H.; Qian, L.; Wang, Y. A comprehensive study on the pyrolysis behavior of pine sawdust catalyzed by different metal ions under conventional and microwave heating conditions. *Energy* **2023**, *272*, 127115. [CrossRef]
39. Ellison, C.R.; Hoff, R.; Mărculescu, C.; Boldor, D. Investigation of microwave-assisted pyrolysis of biomass with char in a rectangular waveguide applicator with built-in phase-shifting. *Appl. Energy* **2020**, *259*, 114217. [CrossRef]
40. Du, H.; Zhong, Z.; Zhang, B.; Shi, K.; Li, Z. Ex-situ catalytic upgrading of vapors from microwave-assisted pyrolysis of bamboo with chemical liquid deposition modified HZSM-5 to enhance aromatics production. *J. Anal. Appl. Pyrolysis* **2020**, *149*, 104857. [CrossRef]
41. Kaewtrakulchai, N.; Faungnawakij, K.; Eiad-Ua, A. Parametric Study on Microwave-Assisted Pyrolysis Combined KOH Activation of Oil Palm Male Flowers Derived Nanoporous Carbons. *Material* **2020**, *13*, 2876. [CrossRef]
42. An, Y.; Tahmasebi, A.; Zhao, X.; Matamba, T.; Yu, J. Catalytic reforming of palm kernel shell microwave pyrolysis vapors over iron-loaded activated carbon: Enhanced production of phenol and hydrogen. *Bioresour. Technol.* **2020**, *306*, 123111. [CrossRef] [PubMed]
43. Idris, R.; Chong, W.W.F.; Ali, A.; Idris, S.; Hasan, M.F.; Ani, F.N.; Chong, C.T. Phenol-rich bio-oil derivation via microwave-induced fast pyrolysis of oil palm empty fruit bunch with activated carbon. *Environ. Technol. Innov.* **2021**, *21*, 101291. [CrossRef]
44. Halim, S.A.; Mohd, N.A.; Razali, N.A. A comparative assessment of biofuel products from rice husk and oil palm empty fruit bunch obtained from conventional and microwave pyrolysis. *J. Taiwan Inst. Chem. Eng.* **2022**, *134*, 104305. [CrossRef]
45. Sahoo, D.; Remya, N. Influence of operating parameters on the microwave pyrolysis of rice husk: Biochar yield, energy yield, and property of biochar. *Biomass Convers. Biorefin.* **2020**, *12*, 3447–3456. [CrossRef]
46. Sridevi, V.; Suriapparao, D.V.; Tukarambai, M.; Terapalli, A.; Ramesh, P.; Sankar Rao, C.; Gautam, R.; Moorthy, J.V.; Suresh Kumar, C. Understanding of synergy in non-isothermal microwave-assisted in-situ catalytic co-pyrolysis of rice husk and polystyrene waste mixtures. *Bioresour. Technol.* **2022**, *360*, 127589. [CrossRef] [PubMed]
47. Zhao, Y.; Liu, B.; Zhang, L.; Guo, S. Microwave Pyrolysis of Macadamia Shells for Efficiently Recycling Lithium from Spent Lithium-ion Batteries. *J. Hazard. Mater.* **2020**, *396*, 122740. [CrossRef]
48. Liu, C.; Liu, X.; He, Y.; An, X.; Fan, D.; Wu, Z. Microwave-assisted catalytic pyrolysis of apple wood to produce biochar: Co-pyrolysis behavior, pyrolysis kinetics analysis and evaluation of microbial carriers. *Bioresour. Technol.* **2021**, *320*, 124345. [CrossRef] [PubMed]
49. Li, M.; Yu, Z.; Bin, Y.; Huang, Z.; He, H.; Liao, Y.; Zheng, A.; Ma, X. Microwave-assisted pyrolysis of eucalyptus wood with MoO3 and different nitrogen sources for coproducing nitrogen-rich bio-oil and char. *J. Anal. Appl. Pyrolysis* **2022**, *167*, 105666. [CrossRef]
50. Zhang, Z.; Huang, K.; Mao, C.; Huang, J.; Xu, Q.; Liao, L.; Wang, R.; Chen, S.; Li, P.; Zhang, C. Microwave assisted catalytic pyrolysis of bagasse to produce hydrogen. *Int. J. Hydrogen Energy* **2022**, *47*, 35626–35634. [CrossRef]
51. Allende, S.; Brodie, G.; Jacob, M.V. Energy recovery from sugarcane bagasse under varying microwave-assisted pyrolysis conditions. *Bioresour. Technol. Rep.* **2022**, *20*, 101283. [CrossRef]
52. Li, K.; Chen, G.; Chen, J.; Peng, J.; Ruan, R.; Srinivasakannan, C. Microwave pyrolysis of walnut shell for reduction process of low-grade pyrolusite. *Bioresour. Technol.* **2019**, *291*, 121838. [CrossRef] [PubMed]
53. Zhu, Y.; Xu, G.; Song, W.; Zhao, Y.; Miao, Z.; Yao, R.; Gao, J. Catalytic microwave pyrolysis of orange peel: Effects of acid and base catalysts mixture on products distribution. *J. Energy Inst.* **2021**, *98*, 172–178. [CrossRef]
54. Chen, L.; Mi, B.; He, J.; Li, Y.; Zhou, Z.; Wu, F. Functionalized biochars with highly-efficient malachite green adsorption property produced from banana peels via microwave-assisted pyrolysis. *Bioresour. Technol.* **2023**, *376*, 128840. [CrossRef]

55. Mathiarasu, A.; Pugazhvadivu, M. Studies on dielectric properties and microwave pyrolysis of karanja seed. *Biomass Convers. Biorefin.* **2021**, *13*, 2895–2905. [CrossRef]
56. Elnajjar, E.; Syam, M.M.; Al-Omari, S.A.B. Experimental investigations of bio-syngas production using microwave pyrolysis of UAE'S palm date seed pits. *Fuel* **2021**, *303*, 121348. [CrossRef]
57. Fan, S.; Zhang, Y.; Cui, L.; Maqsood, T.; Nižetić, S. Cleaner production of aviation oil from microwave-assisted pyrolysis of plastic wastes. *J. Clean. Prod.* **2023**, *390*, 136102. [CrossRef]
58. Sardi, B.; Rachmawati, H.; Maulana, T.F.; Setiawati, E.; Indrawan, N.; Mahfud, M. Advanced bio-oil production from a mixture of microalgae and low rank coal using microwave assisted pyrolysis. *Bioresour. Technol. Rep.* **2023**, *21*, 101367. [CrossRef]
59. Yang, X.; Ke, L.; Wu, Q.; Cui, X.; Zhang, Q.; Tian, X.; Zeng, Y.; Cobb, K.; Liu, Y.; Ruan, R.; et al. Microwave-assisted pyrolysis spent bleaching clay for aromatic bio-oil production: Exploration of heating pathway based on microwave response characteristics of feedstock. *J. Anal. Appl. Pyrolysis* **2022**, *167*, 105685. [CrossRef]
60. Wang, Y.; Zeng, Y.; Fan, L.; Wu, Q.; Zhang, L.; Xiong, J.; Zhang, J.; Liao, R.; Cobb, K.; Liu, Y.; et al. Pyrolysis of different types of waste cooking oil in the presence/absence HZSM-5 catalyst: Influence of feedstock characteristics on aromatic formation. *Fuel* **2023**, *351*, 128937. [CrossRef]
61. Wu, Q.; Zhang, L.; Ke, L.; Zhang, Q.; Cui, X.; Yang, Q.; Wang, Y.; Dai, A.; Xu, C.; Liu, Y.; et al. Microwave-assisted pyrolysis of waste cooking oil for bio-based hydrocarbons over Chem-CaO@SiC catalyst. *Energy* **2023**, *263*, 125683. [CrossRef]
62. Zou, R.; Wang, C.; Qian, M.; Huo, E.; Kong, X.; Wang, Y.; Dai, L.; Wang, L.; Zhang, X.; Mateo, W.C.; et al. Catalytic co-pyrolysis of solid wastes (low-density polyethylene and lignocellulosic biomass) over microwave assisted biochar for bio-oil upgrading and hydrogen production. *J. Clean. Prod.* **2022**, *374*, 133971. [CrossRef]
63. Fan, S.; Zhang, Y.; Cui, L.; Xiong, Q.; Maqsood, T. Conversion of Polystyrene Plastic into Aviation Fuel through Microwave-Assisted Pyrolysis as Affected by Iron-Based Microwave Absorbents. *ACS Sustain. Chem. Eng.* **2023**, *11*, 1054–1066. [CrossRef]
64. Suriapparao, D.V.; Reddy, B.R.; Rao, C.S.; Jeeru, L.R.; Kumar, T.H. Prosopis juliflora valorization via microwave-assisted pyrolysis: Optimization of reaction parameters using machine learning analysis. *J. Anal. Appl. Pyrolysis* **2023**, *169*, 105811. [CrossRef]
65. Cui, Y.; Zhang, Y.; Cui, L.; Liu, Y.; Li, B.; Liu, W. Microwave-assisted pyrolysis of polypropylene plastic for liquid oil production. *J. Clean. Prod.* **2023**, *411*, 137303. [CrossRef]
66. Liu, J.; Hou, Q.; Ju, M.; Ji, P.; Sun, Q.; Li, W. Biomass Pyrolysis Technology by Catalytic Fast Pyrolysis, Catalytic Co-Pyrolysis and Microwave-Assisted Pyrolysis: A Review. *Catalysts* **2020**, *10*, 742. [CrossRef]
67. Wang, J.; Zhong, Z.; Song, Z.; Ding, K.; Deng, A. Modification and regeneration of HZSM-5 catalyst in microwave assisted catalytic fast pyrolysis of mushroom waste. *Energy Convers. Manag.* **2016**, *123*, 29–34. [CrossRef]
68. State, R.N.; Volceanov, A.; Muley, P.; Boldor, D. A review of catalysts used in microwave assisted pyrolysis and gasification. *Bioresour. Technol.* **2019**, *277*, 179–194. [CrossRef]
69. Zhou, Y.; Hu, C. Catalytic Thermochemical Conversion of Algae and Upgrading of Algal Oil for the Production of High-Grade Liquid Fuel: A Review. *Catalysts* **2020**, *10*, 145. [CrossRef]
70. Chen, X.; Li, S.; Liu, Z.; Chen, Y.; Yang, H.; Wang, X.; Che, Q.; Chen, W.; Chen, H. Pyrolysis characteristics of lignocellulosic biomass components in the presence of CaO. *Bioresour. Technol.* **2019**, *287*, 121493. [CrossRef]
71. Arpia, A.A.; Chen, W.-H.; Ubando, A.T.; Tabatabaei, M.; Lam, S.S.; Culaba, A.B.; De Luna, M.D.G. Catalytic microwave-assisted torrefaction of sugarcane bagasse with calcium oxide optimized via Taguchi approach: Product characterization and energy analysis. *Fuel* **2021**, *305*, 121543. [CrossRef]
72. Li, H.; Wang, Y.; Zhou, N.; Dai, L.; Deng, W.; Liu, C.; Cheng, Y.; Liu, Y.; Cobb, K.; Chen, P.; et al. Applications of calcium oxide–based catalysts in biomass pyrolysis/gasification—A review. *J. Clean. Prod.* **2021**, *291*, 125826. [CrossRef]
73. Lin, Y.; Zhang, C.; Zhang, M.; Zhang, J. Deoxygenation of Bio-oil during Pyrolysis of Biomass in the Presence of CaO in a Fluidized-Bed Reactor. *Energy Fuels* **2010**, *24*, 5686–5695. [CrossRef]
74. Ding, K.; Zhong, Z.; Wang, J.; Zhang, B.; Fan, L.; Liu, S.; Wang, Y.; Liu, Y.; Zhong, D.; Chen, P.; et al. Improving hydrocarbon yield from catalytic fast co-pyrolysis of hemicellulose and plastic in the dual-catalyst bed of CaO and HZSM-5. *Bioresour. Technol.* **2018**, *261*, 86–92. [CrossRef]
75. Wang, D.; Xiao, R.; Zhang, H.; He, G. Comparison of catalytic pyrolysis of biomass with MCM-41 and CaO catalysts by using TGA–FTIR analysis. *J. Anal. Appl. Pyrolysis* **2010**, *89*, 171–177. [CrossRef]
76. Lu, Q.; Zhang, Z.-F.; Dong, C.-Q.; Zhu, X.-F. Catalytic Upgrading of Biomass Fast Pyrolysis Vapors with Nano Metal Oxides: An Analytical Py-GC/MS Study. *Energies* **2010**, *3*, 1805–1820. [CrossRef]
77. Wang, H.; Mo, W.; He, X.; Fan, X.; Ma, F.; Liu, S.; Tax, D. Effect of Ca Promoter on the Structure, Performance, and Carbon Deposition of Ni-$Al(_2)O(_3)$ Catalyst for $CO(_2)$-$CH(_4)$ Reforming. *ACS Omega* **2020**, *5*, 28955–28964. [CrossRef]
78. Yi, L.; Liu, H.; Li, M.; Man, G.; Yao, H. Prevention of CaO deactivation using organic calcium precursor during multicyclic catalytic upgrading of bio-oil. *Fuel* **2020**, *271*, 117692. [CrossRef]
79. Gupta, J.; Papadikis, K.; Konysheva, E.Y.; Lin, Y.; Kozhevnikov, I.V.; Li, J. CaO catalyst for multi-route conversion of oakwood biomass to value-added chemicals and fuel precursors in fast pyrolysis. *Appl. Catal. B Environ.* **2021**, *285*, 119858. [CrossRef]
80. Kumagai, S.; Yamasaki, R.; Kameda, T.; Saito, Y.; Watanabe, A.; Watanabe, C.; Teramae, N.; Yoshioka, T. Aromatic hydrocarbon selectivity as a function of CaO basicity and aging during CaO-catalyzed PET pyrolysis using tandem μ-reactor-GC/MS. *Chem. Eng. J.* **2018**, *332*, 169–173. [CrossRef]

81. Castello, D.; He, S.; Ruiz, M.P.; Westerhof, R.J.M.; Heeres, H.J.; Seshan, K.; Kersten, S.R.A. Is it possible to increase the oil yield of catalytic pyrolysis of biomass? A study using commercially-available acid and basic catalysts in ex-situ and in-situ modus. *J. Anal. Appl. Pyrolysis* **2019**, *137*, 77–85. [CrossRef]
82. Huang, Y.F.; Chiueh, P.T.; Kuan, W.H.; Lo, S.L. Microwave pyrolysis of rice straw: Products, mechanism, and kinetics. *Bioresour. Technol.* **2013**, *142*, 620–624. [CrossRef] [PubMed]
83. Shang, H.; Lu, R.-R.; Shang, L.; Zhang, W.-H. Effect of additives on the microwave-assisted pyrolysis of sawdust. *Fuel Process. Technol.* **2015**, *131*, 167–174. [CrossRef]
84. Mamaeva, A.; Tahmasebi, A.; Tian, L.; Yu, J. Microwave-assisted catalytic pyrolysis of lignocellulosic biomass for production of phenolic-rich bio-oil. *Bioresour. Technol.* **2016**, *211*, 382–389. [CrossRef] [PubMed]
85. Zhang, Y.; Chen, P.; Liu, S.; Peng, P.; Min, M.; Cheng, Y.; Anderson, E.; Zhou, N.; Fan, L.; Liu, C.; et al. Effects of feedstock characteristics on microwave-assisted pyrolysis—A review. *Bioresour. Technol.* **2017**, *230*, 143–151. [CrossRef]
86. Subramanian, K.A. A comparison of water–diesel emulsion and timed injection of water into the intake manifold of a diesel engine for simultaneous control of NO and smoke emissions. *Energy Convers. Manag.* **2011**, *52*, 849–857. [CrossRef]
87. Chen, X.; Chen, Y.; Yang, H.; Wang, X.; Che, Q.; Chen, W.; Chen, H. Catalytic fast pyrolysis of biomass: Selective deoxygenation to balance the quality and yield of bio-oil. *Bioresour. Technol.* **2019**, *273*, 153–158. [CrossRef]
88. Mirghiasi, Z.; Bakhtiari, F.; Darezereshki, E.; Esmaeilzadeh, E. Preparation and characterization of CaO nanoparticles from Ca(OH)2 by direct thermal decomposition method. *J. Ind. Eng. Chem.* **2014**, *20*, 113–117. [CrossRef]
89. Correia, L.M.; Saboya, R.M.A.; de Sousa Campelo, N.; Cecilia, J.A.; Rodríguez-Castellón, E.; Cavalcante, C.L.; Vieira, R.S. Characterization of calcium oxide catalysts from natural sources and their application in the transesterification of sunflower oil. *Bioresour. Technol.* **2014**, *151*, 207–213. [CrossRef]
90. Goli, J.; Sahu, O. Development of heterogeneous alkali catalyst from waste chicken eggshell for biodiesel production. *Renew. Energy* **2018**, *128*, 142–154. [CrossRef]
91. Lesbani, A.; Tamba, P.; Mohadi, R.; Fahmariyanti, F. Preparation of calcium oxide from Achatina Fulica as catalyst for production of biodiesel from waste cooking oil. *Indones. J. Chem.* **2013**, *13*, 176–180. [CrossRef]
92. Zhang, C.; Hu, X.; Guo, H.; Wei, T.; Dong, D.; Hu, G.; Hu, S.; Xiang, J.; Liu, Q.; Wang, Y. Pyrolysis of poplar, cellulose and lignin: Effects of acidity and alkalinity of the metal oxide catalysts. *J. Anal. Appl. Pyrolysis* **2018**, *134*, 590–605. [CrossRef]
93. Hu, M.; Zhang, H.; Ye, Z.; Ma, J.; Chen, Z.; Wang, J.; Wang, C.; Pan, Z. Thermogravimetric kinetics and pyrolytic tri-state products analysis towards insights into understanding the pyrolysis mechanism of Spirulina platensis with calcium oxide. *Renew. Energy* **2022**, *184*, 498–509. [CrossRef]
94. Wang, Q.; Zhang, X.; Sun, S.; Wang, Z.; Cui, D. Effect of CaO on Pyrolysis Products and Reaction Mechanisms of a Corn Stover. *ACS Omega* **2020**, *5*, 10276–10287. [CrossRef] [PubMed]
95. Chen, X.; Chen, Y.; Yang, H.; Chen, W.; Wang, X.; Chen, H. Fast pyrolysis of cotton stalk biomass using calcium oxide. *Bioresour. Technol.* **2017**, *233*, 15–20. [CrossRef] [PubMed]
96. Liu, S.; Xie, Q.; Zhang, B.; Cheng, Y.; Liu, Y.; Chen, P.; Ruan, R. Fast microwave-assisted catalytic co-pyrolysis of corn stover and scum for bio-oil production with CaO and HZSM-5 as the catalyst. *Bioresour. Technol.* **2016**, *204*, 164–170. [CrossRef]
97. Yongbin, J.; Jiejie, H.; Yang, W. Effects of Calcium Oxide on the Cracking of Coal Tar in the Freeboard of a Fluidized Bed. *Energy Fuels* **2004**, *18*, 1625–1632. [CrossRef]
98. Derringer, G.; Suich, R. Simultaneous Optimization of Several Response Variables. *J. Qual. Technol.* **2018**, *12*, 214–219. [CrossRef]
99. Costa, N.R.; Lourenço, J.; Pereira, Z.L. Desirability function approach: A review and performance evaluation in adverse conditions. *Chemom. Intell. Lab. Syst.* **2011**, *107*, 234–244. [CrossRef]
100. Mantilla, S.V.; Manrique, A.M.; Gauthier-Maradei, P. Methodology for Extraction of Phenolic Compounds of Bio-oil from Agricultural Biomass Wastes. *Waste Biomass Valoriz.* **2015**, *6*, 371–383. [CrossRef]
101. Cardoso, C.R.; Ataíde, C.H. Analytical pyrolysis of tobacco residue: Effect of temperature and inorganic additives. *J. Anal. Appl. Pyrolysis* **2013**, *99*, 49–57. [CrossRef]
102. Fele Žilnik, L.; Jazbinšek, A. Recovery of renewable phenolic fraction from pyrolysis oil. *Sep. Purif. Technol.* **2012**, *86*, 157–170. [CrossRef]
103. McGrath, T.E.; Brown, A.P.; Meruva, N.K.; Chan, W.G. Phenolic compound formation from the low temperature pyrolysis of tobacco. *J. Anal. Appl. Pyrolysis* **2009**, *84*, 170–178. [CrossRef]
104. Case, P.A.; Truong, C.; Wheeler, M.C.; DeSisto, W.J. Calcium-catalyzed pyrolysis of lignocellulosic biomass components. *Bioresour. Technol.* **2015**, *192*, 247–252. [CrossRef] [PubMed]
105. Lu, H.; Khan, A.; Smirniotis, P.G. Relationship between Structural Properties and CO_2 Capture Performance of CaO−Based Sorbents Obtained from Different Organometallic Precursors. *Ind. Eng. Chem. Res.* **2008**, *47*, 6216–6220. [CrossRef]
106. Ding, L.; Rahimi, P.; Hawkins, R.; Bhatt, S.; Shi, Y. Naphthenic acid removal from heavy oils on alkaline earth-metal oxides and ZnO catalysts. *Appl. Catal. A Gen.* **2009**, *371*, 121–130. [CrossRef]
107. Xulai, Y.; Jian, Z.; Xifeng, Z. Decomposition and Calcination Characteristics of Calcium-Enriched Bio-oil. *Energy Fuels* **2008**, *22*, 2598–2603. [CrossRef]
108. Chireshe, F.; Collard, F.-X.; Görgens, J.F. Production of an upgraded bio-oil with minimal water content by catalytic pyrolysis: Optimisation and comparison of CaO and MgO performances. *J. Anal. Appl. Pyrolysis* **2020**, *146*, 104751. [CrossRef]

109. Andrade, L.A.; Barrozo, M.A.S.; Vieira, L.G.M. Thermo-chemical behavior and product formation during pyrolysis of mango seed shell. *Ind. Crops Prod.* **2016**, *85*, 174–180. [CrossRef]
110. Chen, Z.; Hu, M.; Zhu, X.; Guo, D.; Liu, S.; Hu, Z.; Xiao, B.; Wang, J.; Laghari, M. Characteristics and kinetic study on pyrolysis of five lignocellulosic biomass via thermogravimetric analysis. *Bioresour. Technol.* **2015**, *192*, 441–450. [CrossRef] [PubMed]
111. Myers, R.H.; Khuri, A.I.; Carter, W.H. Response Surface Methodology: 1966–l988. *Technometrics* **1989**, *31*, 137–157. [CrossRef]